

Review

Engineering of Plant Polyketide Biosynthesis

Ikuro ABE^{a,b}

^aSchool of Pharmaceutical Sciences, University of Shizuoka; Yada, Shizuoka 422–8526, Japan; and ^bPRESTO, Japan Science and Technology Agency; Kawaguchi, Saitama 332–0012, Japan.

Received June 2, 2008

A growing number of functionally divergent the chalcone synthase (CHS) superfamily type III polyketide synthases (PKSs) have been cloned and characterized, which include recently obtained pentaketide chromone synthase (PCS) and octaketide synthase (OKS) from aloe (*Aloe arborescens*). Recombinant PCS expressed in *Escherichia coli* catalyzes iterative condensations of five molecules of malonyl-CoA to produce a pentaketide, 5,7-dihydroxy-2-methylchromone, while OKS carries out sequential condensations of eight molecules of malonyl-CoA to yield aromatic octaketides, SEK4 and SEK4b, the longest polyketides generated by the structurally simple type III PKS. The two enzymes share 91% amino acid sequence identity, maintaining most of the active-site residues of CHS including the Cys-His-Asn catalytic triad. One of the most characteristic features is that the conserved Thr197 of CHS (numbering in *Medicago sativa* CHS) is uniquely replaced with Met207 in PCS and with Gly207 in OKS, respectively. Site-directed mutagenesis and X-ray crystallographic studies clearly demonstrated that the chemically inert single residue lining the active-site cavity controls the polyketide chain length and the product specificity depending on the steric bulk of the side chain. Finally, on the basis of the crystal structures of both wild-type and M207G-mutant PCS, a triple mutant PCS F80A/Y82A/M207G was constructed and shown to catalyze condensations of nine molecules of malonyl-CoA to produce a novel nonaketide naphthopyrone with a fused tricyclic ring system. Structure-based engineering of the type III PKS superfamily enzymes would thus lead to further production of chemically and structurally divergent unnatural novel polyketides.

Key words biosynthesis; polyphenol; type III polyketide synthase; engineered biosynthesis; protein engineering

1. Introduction

The chalcone synthase (CHS) superfamily of type III polyketide synthases (PKSs) generates a wide variety of plant secondary metabolite scaffolds including chalcone, stilbene, phloroglucinol, resorcinol, benzophenone, biphenyl, chromone, isocoumarin, acridone, quinolinone, pyrone, curcuminoid, etc.^{1,2)} The type III PKSs are structurally and mechanistically different from the modular type I and the dissociated type II PKSs of bacterial origin; the simple homodimer of 40–45 kDa proteins perform a complete series of decarboxylation, condensation, and cyclization reactions with a single active site by utilizing CoA-linked substrates without involvement of the acyl carrier proteins.³⁾ For example, CHS, the ubiquitous plant-specific type III PKS, catalyzes a sequential condensation of the C₆–C₃ unit of *p*-coumaroyl-CoA with three C₂ units from malonyl-CoA to produce naringenin chalcone, the biosynthetic precursor of flavonoids (Fig. 1). The enzyme reaction is initiated by loading of the coumaroyl starter at the active-site Cys residue, which is followed by three rounds of decarboxylative condensation of malonyl-CoA. Finally, cyclization of the enzyme-bound tetraketide intermediate leads to the formation of the new aromatic ring system.^{4–17)}

A growing number of functionally divergent plant type III PKSs including stilbene synthase (STS),^{18,19)} acridone synthase (ACS),^{20–23)} benzalacetone synthase (BAS),^{24–28)} 2-pyrone synthase (2PS),^{29,30)} and aloesone synthase (ALS)^{31,32)}

have been cloned and characterized (Fig. 1). In addition, several bacterial type III PKSs such as 1,3,6,8-tetrahydroxynaphthalene synthase (THNS or RppA) have been also reported.^{33–36)} Recent crystallographic and site-directed mutagenesis studies on the plant and bacterial type III PKSs have revealed that the CHS superfamily enzymes share a common three-dimensional overall fold with an absolutely conserved Cys-His-Asn catalytic triad. The polyketide formation reaction is initiated by a starter molecule loading at the active-site Cys, which is followed by iterative decarboxylative condensations of malonyl-CoA and the final cyclization of the enzyme-bound intermediate (Fig. 2).^{4,18,30)} Most importantly, the enzyme uses a single catalytic Cys, and each chain elongation step involves cleavage of the once formed C–S thioester bond and the subsequent formation of a new C–C bond by the insertion of an additional C₂ building block to produce a CoA-linked polyketide intermediate. The remarkable functional diversity of the CHS superfamily enzymes thus derives from the differences in the selection of the starter molecules, the number of the malonyl-CoA condensations, and the mechanisms of cyclization reactions.

2. Novel PKSs from the Aloe Plant

Pentaketide chromone synthase (PCS)³⁷⁾ and octaketide synthase (OKS)³⁸⁾ are novel plant-specific type III PKSs that catalyze iterative condensations of five and eight molecules of malonyl-CoA, respectively (Fig. 3). The two enzymes

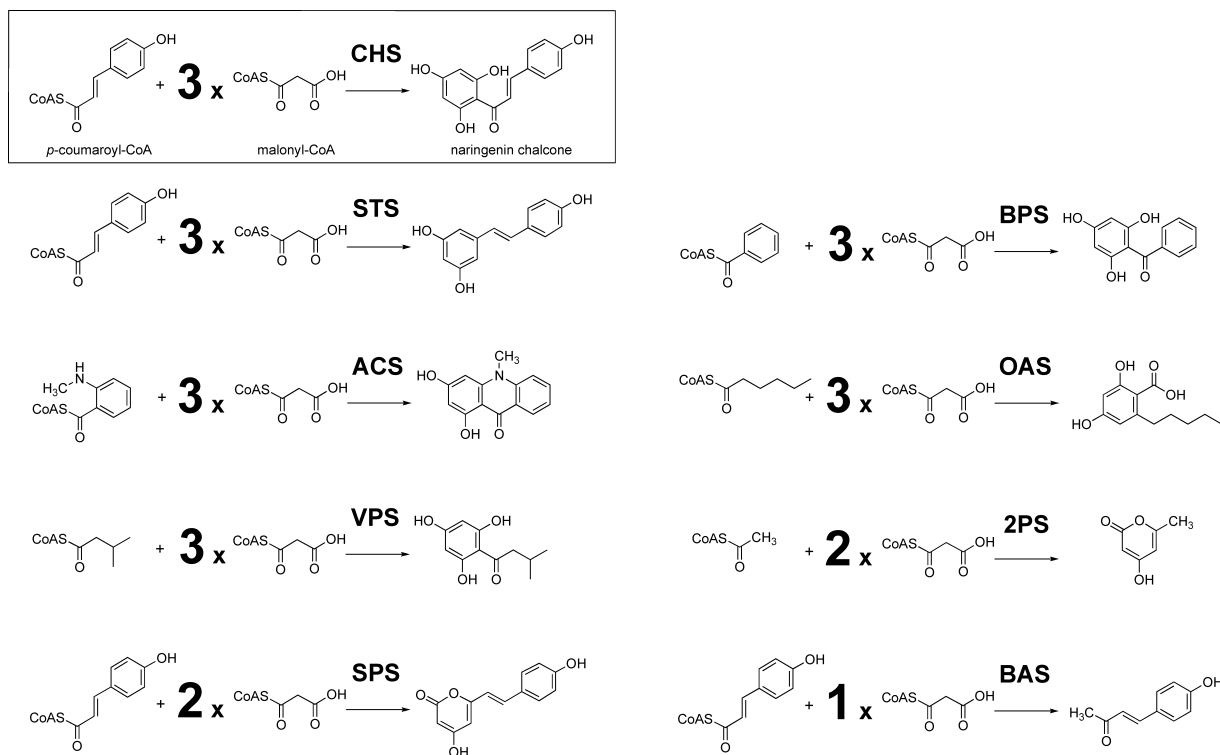


Fig. 1. Biosynthesis of Plant Polyketides by CHS-Superfamily Type III Polyketide Synthases

CHS, chalcone synthase; STS, stilbene synthase; ACS, acridone synthase; VPS, valerophenone synthase; SPS, styrylpyrone synthase; BPS, benzophenone synthase; OAS, olive-tolic acid synthase; 2PS, 2-pyrone synthase; BAS, benzalacetone synthase.

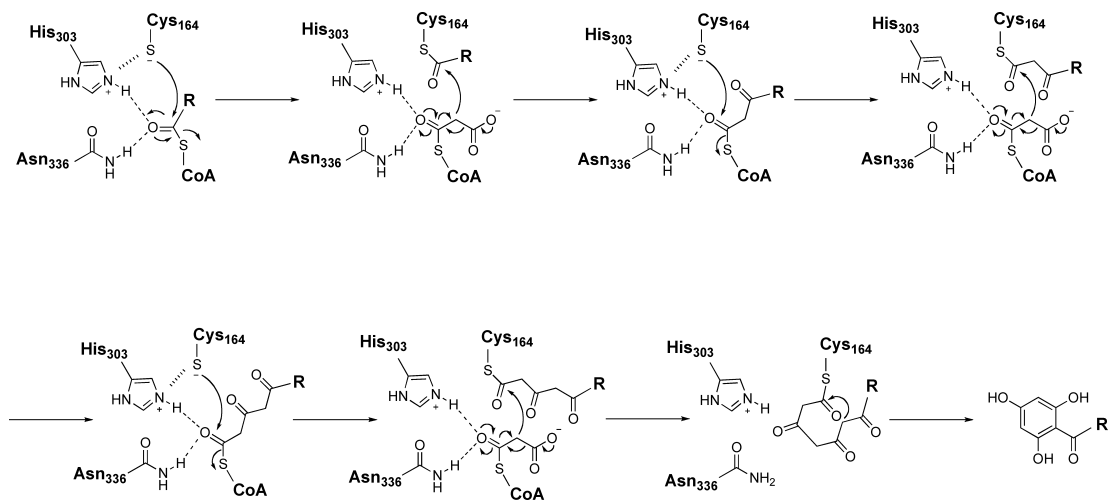


Fig. 2. Proposed Mechanism of the Enzyme Reactions of Type III Polyketide Synthases

Ikuro Abe graduated from The University of Tokyo in 1984 and obtained his Ph.D. in 1989 from the same university under the direction of Professor Yutaka Ebizuka, where he studied the chemistry and biochemistry of natural product biosynthesis. After two years of postdoctoral research with Professor Guy Ourisson at the CNRS Institut de Chimie des Substances Naturelles, and mostly with Professor Michel Rohmer at the Ecole Nationale Supérieure de Chimie de Mulhouse (1989–1991), he moved to the U.S.A. to work with Professor Glenn D. Prestwich at the State University of New York at Stony Brook (1991–1996) and the University of Utah (1996–1998) as a Research Assistant Professor. In 1998, he moved back to Japan to the University of Shizuoka School of Pharmaceutical Sciences. He is currently an Associate Professor and an investigator in PRESTO, Japan Science and Technology Agency (2005–2009). His research interests involve exploring and engineering the biosynthesis of natural products.



Ikuro Abe

were cloned and sequenced from aloe (*Aloe arborescens*), a medicinal plant rich in aromatic polyketides such as pharmaceutically important aloenin (hexaketide), aloesin (heptaketide), and barbaloin (octaketide) (Fig. 4A). Recombinant PCS expressed in *Escherichia coli* does not produce chalcone from *p*-coumaroyl-CoA, but instead efficiently accepts malonyl-CoA as a sole substrate to carry out iterative condensations of five molecules of malonyl-CoA, producing a pentaketide, 5,7-dihydroxy-2-methylchromone (Fig. 3A). The aromatic pentaketide is a biosynthetic precursor of the well known antiasthmatic furochromones, kehellin and visnagin (Fig. 4B).³⁷ On the other hand, recombinant OKS catalyzes sequential condensations of eight molecules of malonyl-CoA to yield a 1:4 mixture of aromatic octaketides, SEK4 and SEK4b, which are the longest polyketides generated by the structurally simple type III PKS (Fig. 3B).³⁸ The octaketides SEK4/SEK4b are known to be the shunt products of the minimal type II PKS for actinorhodin (*act* from *Streptomyces coelicolor*, a heterodimeric complex of ketosynthase

and chain length factor).^{39,40} Since the aloe plant does not produce the octaketides SEK4/SEK4b and their metabolites and is a rich source of anthrones and anthraquinones (octaketides), it is tempting to speculate that OKS is originally involved in the biosynthesis of anthrones and anthraquinones in the medicinal plant. However, maybe because of misfolding of the heterologously expressed recombinant proteins in *E. coli*, or because of the absence of interacting proteins of such as yet unidentified ketoreductase,³⁸ the enzyme possibly yielded SEK4/SEK4b as derailed shunt products just as in the case of the minimal type II PKS (Fig. 4C). The physiological function of OKS in the medicinal plant remains to be elucidated.

Interestingly, both recombinant PCS and OKS accept acetyl-CoA, resulting from decarboxylation of malonyl-CoA, as a starter substrate.^{37,38} This was confirmed by the ¹⁴C incorporation rate from [1-¹⁴C]acetyl CoA in the presence of cold malonyl-CoA, while the yield from [2-¹⁴C]malonyl-CoA was retained at almost the same level either in the pres-

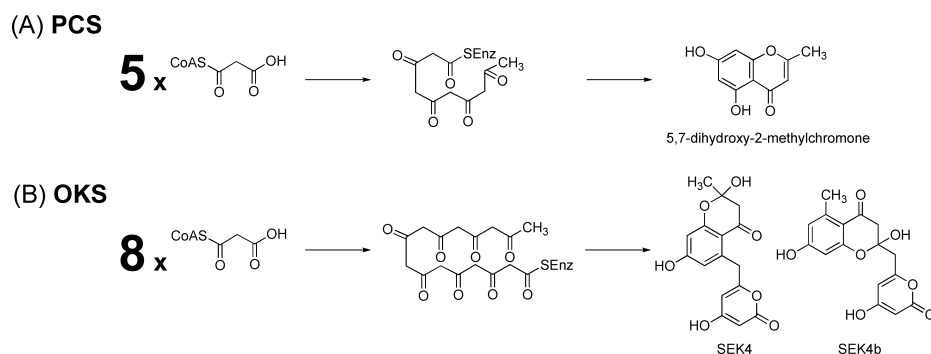


Fig. 3. Proposed Mechanism of the Formation of (A) 5,7-Dihydroxy-2-methylchromone by *A. arborescens* PCS and (B) SEK4/SEK4b by *A. arborescens* OKS

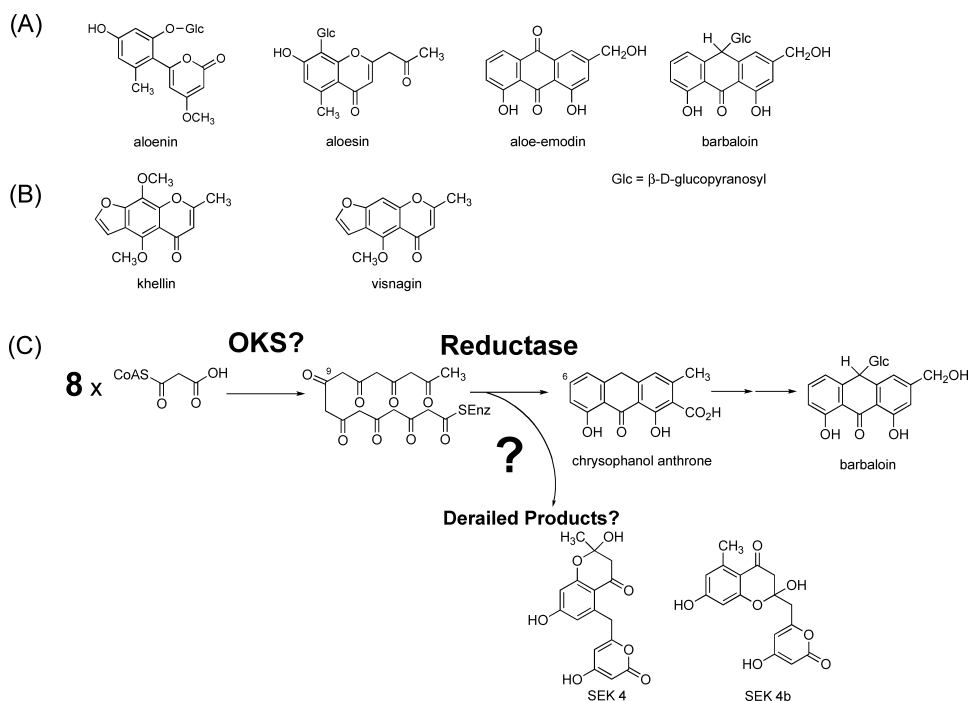


Fig. 4. (A) Structures of Aromatic Polyketides Produced by *A. arborescens*, (B) Structures of Khellin and Visnagin and (C) a Hypothetical Scheme for the Involvement of OKS and as yet Unidentified Ketoreductase in the Biosynthesis of Anthrones and Anthraquinones

In the absence of the reductase, OKS only affords SEK4/SEK4b as derailed products.

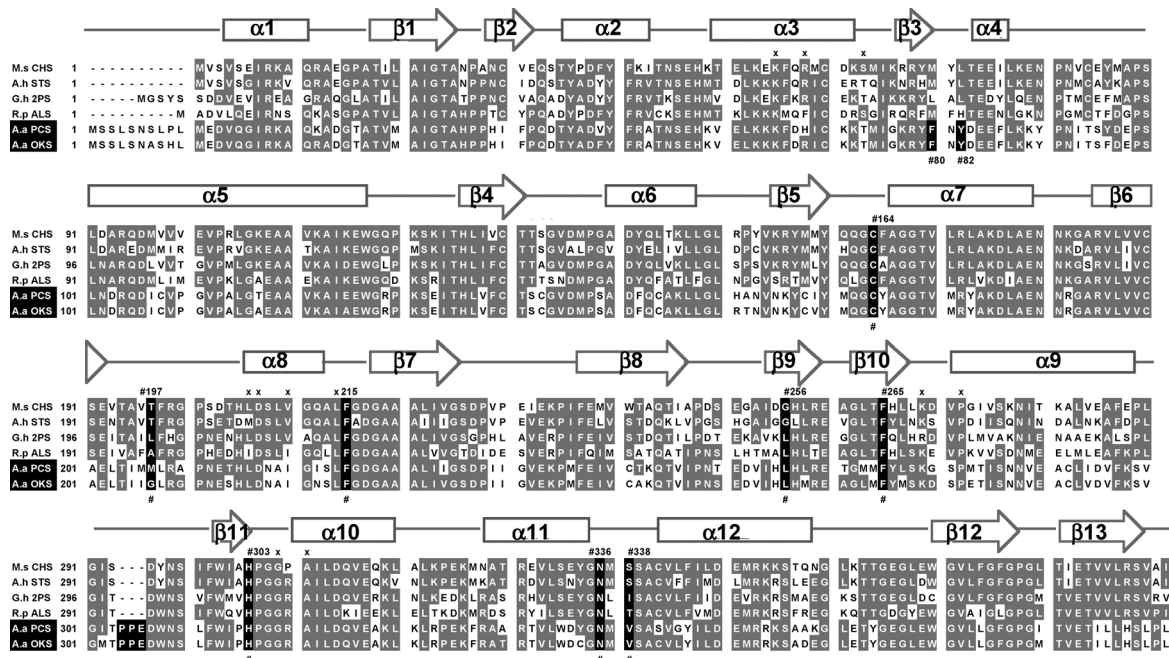


Fig. 5. Comparison of the Amino Acid Sequences of *A. arborescens* PCS and OKS with Other CHS Superfamily Type III PKSs

M.s CHS, *M. sativa* CHS; A.h STS, *Arachis hypogaea* stilbene synthase; G.h 2PS, *G. hybrida* 2PS; R.p ALS, *R. palmatum* ALS; A.a PCS, *A. arborescens* PCS; A.a OKS, *A. arborescens* OKS. The critical active-site residue 197, the catalytic triad (Cys164, His303, and Asn336), and the residues lining the active-site (Phe215, Gly256, F265, Ser338) are marked with # (numbering in *M. sativa* CHS), and residues for the CoA binding with +. Phe80 and Tyr82 of *A. arborescens* PCS are also marked. α -Helices (rectangles) and β -strands (arrows) of CHS are diagrammed.

ence or absence of cold acetyl-CoA. The steady-state kinetics analysis revealed that the recombinant PCS showed a K_M value of $71.0 \mu\text{M}$ and k_{cat} value of $445 \times 10^{-3} \text{min}^{-1}$, with a broad pH optimum within a range of 6.0–8.0, while OKS showed a K_M value of $95.0 \mu\text{M}$ and k_{cat} value of $94.0 \times 10^{-3} \text{min}^{-1}$ for malonyl-CoA with a pH optimum at 7.5. Further, as is the case for other type III PKSs, both PCS and OKS also exhibit extremely broad substrate tolerance; the two enzymes readily accept aromatic (*p*-coumaroyl, cinnamoyl, phenylacetyl, and benzoyl) and aliphatic (C_4 to C_{20} alkyl chain length) CoA thioesters as a starter substrate and carry out up to three condensations with malonyl-CoA to produce triketide and tetraketide α -pyrones as major products.^{37,38} In particular, it is noteworthy that OKS efficiently accepts *n*-eicosanoyl (C_{20}) CoA to produce the α -pyrones, while regular CHS only accepts up to the C_{12} chain length CoA thioester. Furthermore, OKS also readily accepts (2*RS*)-methylmalonyl-CoA as a sole substrate (both as a “starter” and an “extender”) to produce an unnatural methylated C_9 triketide α -pyrone, 6-ethyl-4-hydroxy-3,5-dimethyl-2-pyrone, by sequential decarboxylative condensations of three molecules of (2*RS*)-methylmalonyl-CoA.⁴¹

3. Sequence Analysis

The deduced amino acid sequences of PCS and OKS (*Mr* 44 kDa proteins with 403 amino acids) are 91% identical (368/403), and show 50–60% identity to those of other CHS superfamily type III PKSs of plant origin; OKS shares 60% identity (240/403) with CHS from alfalfa (*Medicago sativa*),⁴ and 54% identity (216/403) with a heptaketide-producing aloesone synthase (ALS) from rhubarb (*Rheum palmatum*)³¹ (Fig. 5). In contrast, PCS and OKS show only relatively low sequence similarity with type III PKSs of bac-

terial origin; OKS shares only 23% identity (93/403) with 1,3,6,8-tetrahydroxynaphthalene synthase (THNS or RppA) from *Streptomyces griseus*.³³

The phylogenetic tree analyses (Fig. 6) demonstrated that the pentaketide-producing PCS and the octaketide-producing OKS from *A. arborescens* (Liliaceae) were grouped with other non-chalcone forming enzymes such as bibenzyl synthase (BBS) from *Phalaenopsis* sp. (Orchidaceae),⁴² ACS from *Ruta graveolens* (Rutaceae),²⁰ 2PS from *Gerbera hybrida* (Asteraceae),²⁹ two CHS-like enzymes with unknown function from *Ipomoea purpurea* (Convolvulaceae),⁴³ and the heptaketide-producing ALS from *R. palmatum* (Polygonaceae).³¹ Interestingly, STS, grouped with the CHS from the same or related plants, has been proposed to have evolved independently several times from CHS.⁴⁴

Comparison of the amino acid sequences revealed that *A. arborescens* PCS and OKS maintain most of the CHS active-site residues (Met137, Gly211, Gly216, Pro375, and the CHS “gatekeepers” Phe215 and Phe265) as well as the catalytic triad (Cys164, His303, and Asn336) (numbering in *M. sativa* CHS)⁴ (Fig. 5). On the other hand, the conserved active-site residues of CHS, Thr197, Gly256, and Ser338, are uniquely replaced in PCS (T197M/G256L/S338V) and in OKS (T197G/G256L/S338V).^{37,38} The chemically inert residues lining the active-site cavity are sterically altered in a number of functionally different type III PKSs as is the case for the triketide-producing *G. hybrida* 2PS (T197L/G256L/S338I),³⁰ and the heptaketide-producing *R. palmatum* ALS (T197A/G256L/S338T).³² On the basis of the crystal structures of *M. sativa* CHS and *G. hybrida* 2PS, Noel and coworkers proposed that the residues play a crucial role for controlling starter substrate selectivity and polyketide chain length by steric modulation of the active-site cavity.³⁰ A

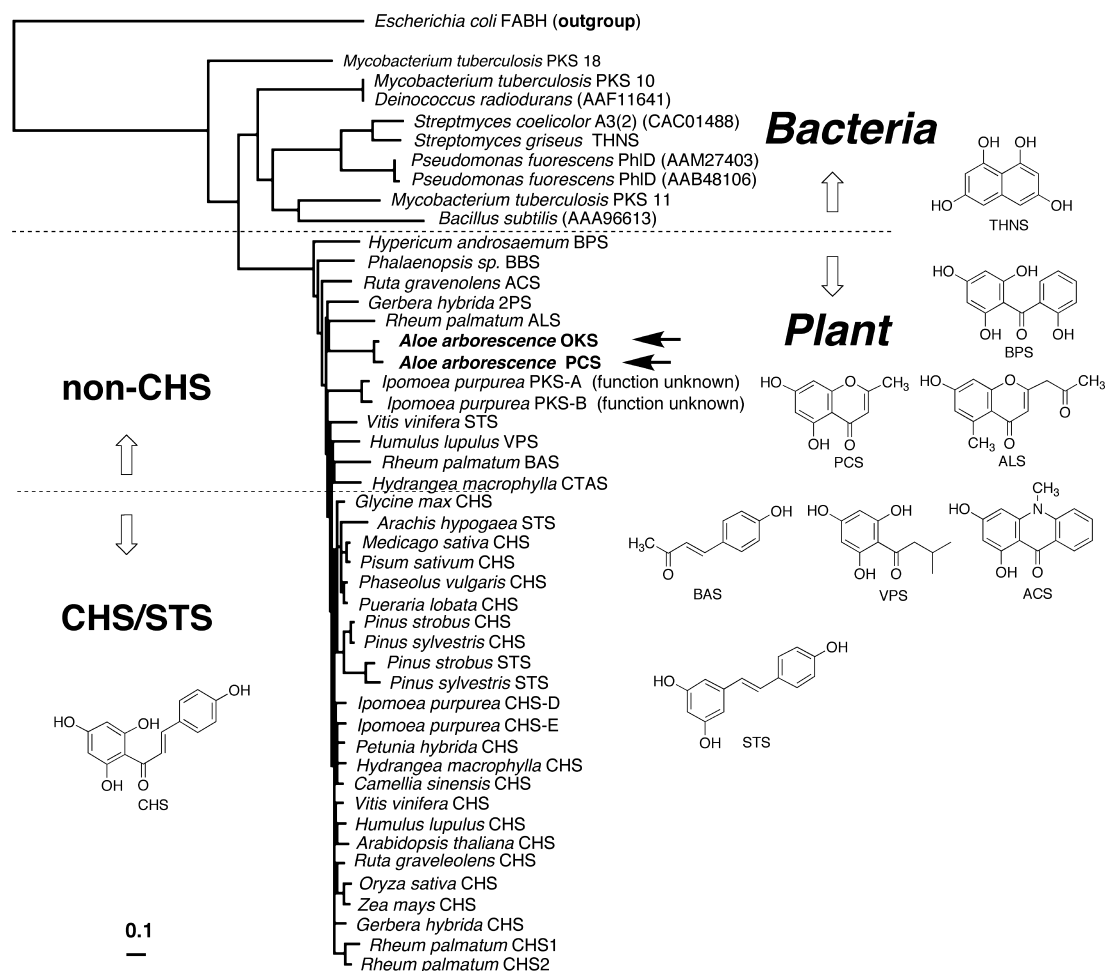


Fig. 6. Phylogenetic Tree Analyses of the CHS Superfamily Type III PKSs

The indicated scale represents 0.1 amino acid substitution per site. Multiple sequence alignment was performed using CLUSTAL W (1.8) and the tree was constructed using the majority rule and strict consensus algorithm implanted in PHYLIP. CHS, chalcone synthase; STS, stilbene synthase; 2PS, 2-pyrone synthase; ACS, acridone synthase; ALS, aloesone synthase; BBS, bibenzyl synthase; BPS, benzophenone synthase; OKS, octaketide synthase; PCS, pentaketide chromone synthase; CTAS, *p*-coumaroyltriatic acid synthase; BAS, benzalacetone synthase; VPS, valerophenone synthase; RppA, red-brown pigment producing enzyme. The β -ketoacyl carrier protein synthase III (FABH) of *E. coli* was employed as an outgroup.

triple mutant of these residues (T197L/G256L/S338I) of *M. sativa* CHS was shown to yield an enzyme that is functionally identical to 2PS.³⁰ Finally, another interesting feature is that both *A. arborescens* PCS and OKS retain a characteristic three-amino acid “PPE” insertion at 10 residues upstream from the catalytic H303 (Fig. 5). A similar insertion has been also reported for coumaroyltriatic acid synthase⁴⁵) (or stilbenecarboxylate synthase⁴⁶) from *Hydrangea macrophylla*, which has a six-amino acid “SIDSII” insertion at the same position.

4. Site-Directed Mutagenesis

Despite the high sequence similarity (91% amino acid sequence identity), PCS and OKS catalyze completely different enzyme reactions. To investigate the structure–function relationship of the pentaketide-producing PCS and the octaketide-producing OKS, we first looked at the conserved residue Thr197 of CHS which is uniquely replaced with bulky Met207 in PCS and with small Gly207 in OKS, respectively (Fig. 5). We constructed a PCS mutant in which Met207 was replaced with Gly as in the case of OKS. To our surprise, the point mutation resulted in a dramatic change in the enzyme activity; the PCS M207G mutant no longer produced the

pentaketide chromone but instead efficiently catalyzed sequential condensations of eight molecules of malonyl-CoA to produce a 1 : 4 mixture of the octaketides SEK4/SEK4b (Fig. 7A).³⁷ The pentaketide-producing PCS was thus transformed into an octaketide synthase by the single-amino acid replacement.

On the contrary, when Gly207 in OKS was substituted with bulky Met as in PCS, the OKS G207M mutant completely lost the octaketide-forming activity, but efficiently produced an unnatural pentaketide, 2,7-dihydroxy-5-methylchromone, from five molecules of malonyl-CoA (Fig. 7B).³⁸ Thus the octaketide-producing OKS was in turn functionally converted to a pentaketide synthase by the small-to-large amino acid substitution. Here it should be noted that the pentaketide product is a regioisomer of the PCS’s 5,7-dihydroxy-2-methylchromone, which is formed by a C-1/C-6 Claisen-type cyclization (Fig. 7A). In the OKS mutant, a C-4/C-9 aldol-type cyclization yielded 2,7-dihydroxy-5-methylchromone. Despite the 91% sequence identity, OKS and PCS are not functionally interconvertible by the single-amino acid switch, suggesting additional subtle structural differences of the active-site architecture between the two enzymes.

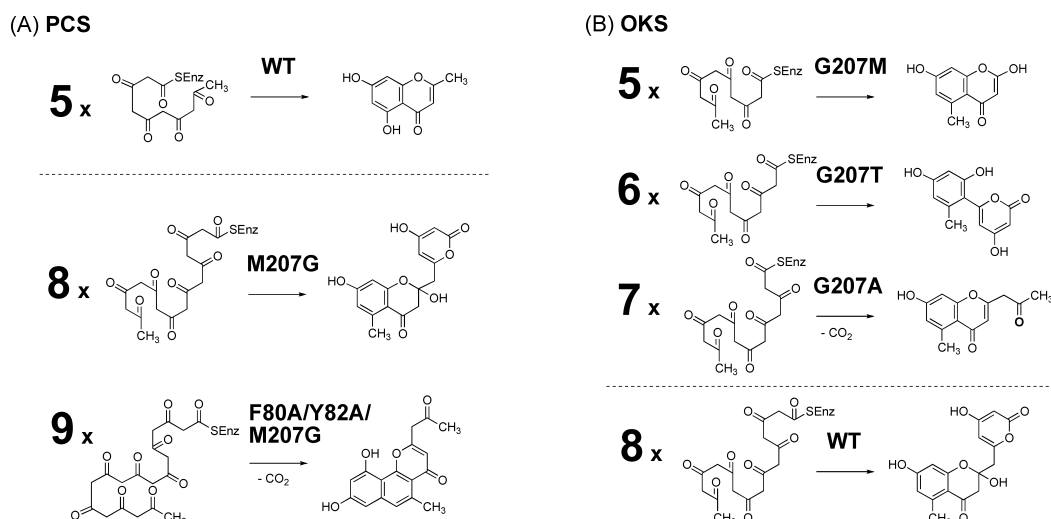


Fig. 7. Proposed Mechanism of the Formation of Unnatural Polyketides by Site-Directed Mutants of *A. arborescens* (A) PCS and (B) OKS

These results clearly suggest that the single residue 207 plays a crucial role in controlling the polyketide chain length and product specificity by simply modulating the size and shape of the active-site cavity. To test further this hypothesis, we constructed a set of *A. arborescens* OKS mutants (G207A, G207T, G207L, G207F, and G207W) and investigated the mechanistic consequences of the point mutations (Fig. 7B).³⁸⁾ First, when Gly207 was replaced with Ala as in the case of the heptaketide-producing *R. palmatum* ALS,³¹⁾ the G207A mutant indeed yielded the heptaketide aloesone in addition to SEK4/SEK4b. Interestingly, the heptaketide is a biosynthetic precursor of aloesin, the antiinflammatory glucoside of the aloe plant (Fig. 4A). Next, when Gly207 was substituted with Thr as in CHS, the G207T mutant lost the octaketide-forming activity and yielded a hexaketide, 6-(2,4-dihydroxy-6-methylphenyl)-4-methoxy-2-pyrone, from six molecules of malonyl-CoA. Notably, the hexaketide is a precursor of aloenin, the antihistaminic glucoside of the medicinal plant (Fig. 4A). Further, other bulky substitutions G207L and G207F yielded the pentaketide 2,7-dihydroxy-5-methylchromone, while the most bulky G207W only afforded a tetraketide, tetracetic acid lactone, along with the triketide, triacetic acid lactone (TAL), without the formation of an aromatic ring system.

It was thus clearly demonstrated that the steric bulk of the chemically inert single residue 207 in *A. arborescens* PCS and OKS (corresponding to Thr197 in *M. sativa* CHS) determines the number of malonyl-CoA condensations. The small-to-large substitutions in place of Gly207 in OKS resulted in loss of the octaketide-producing activity and the concomitant formation of shorter chain length polyketides, ranging from triketide to heptaketide, including the precursors of pharmaceutically important aloenin (hexaketide) and aloesin (heptaketide).³⁸⁾ Presumably, the single-amino acid replacement causes steric contraction of the active-site pocket that accommodates the growing polyketide intermediates, leading to the shortening of the product chain length. It is intriguing that such a simple steric modulation of the active-site cavity causes a dramatic change in the catalytic activity. Mechanistically, OKS and the Gly207 mutants are likely to catalyze the initial aldol-type aromatic ring forma-

tion at the methyl end of the growing polyketide intermediates. The partially cyclized intermediates would be then released from the active site and undergo spontaneous and nonenzymatic α -pyrone ring formations, thereby completing the construction of the fused-ring systems.

5. Crystallographic Analysis

We have resolved the X-ray crystal structures of *A. arborescens* PCS, both the pentaketide-producing wild-type enzyme and the octaketide-producing M207G mutant, at 1.6 Å resolution.^{47,48)} Further, more recently, we have also succeeded in the crystallization of *A. arborescens* OKS.⁴⁹⁾ The X-ray crystallographic analysis revealed that both PCS and OKS share almost the same three-dimensional overall fold with other plant-specific type III PKSs, including the CoA binding tunnel and the active-site architecture of the Cys-His-Asn catalytic triad.⁴⁸⁾ To our surprise, the structural comparison demonstrated that most of the active-site residues of *A. arborescens* PCS and *M. sativa* CHS are superimposable in nearly identical positions. The only exceptions are Cys143, Thr204, Met207, Leu266, and Val351 of *A. arborescens* PCS (corresponding to Ser133, Thr194, Thr197, Gly256, and Ser338 of *M. sativa* CHS, respectively), which accounts for the difference in the catalytic functions of the two enzymes. As described above, the latter three residues, Met207, Leu266, and Val351, altered in a number of functionally divergent type III PKSs, are thought to play critical roles in controlling the substrate and product specificities of the enzyme reactions (Fig. 8). On the other hand, a comparison of the structures with *M. sativa* CHS and *G. hybrida* 2PS revealed a significant backbone change in residues 296–309 of PCS (corresponding to residues 286–296 of *M. sativa* CHS and 291–301 of *G. hybrida* 2PS, respectively), which is due to the characteristic insertion of the three “PPE” residues 304–306, and the addition of 10 residues at the *N*-terminus. Finally, it should be noted that the PCS crystal structure revealed neither a hydrogen bond network nor any additional catalytic Cys residues that appeared to be crucial for the enzyme reaction.

A structural comparison of the wild-type and the M207G mutant PCS revealed that the conformations of the residues

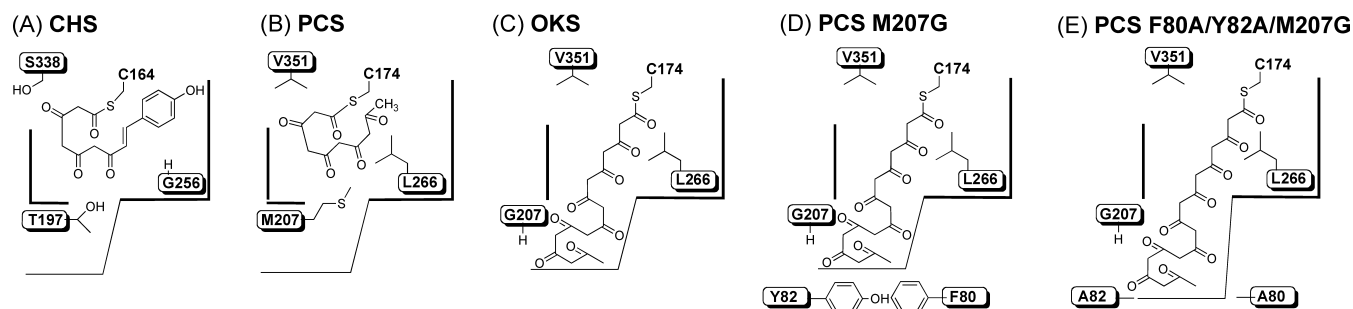


Fig. 8. Schematic Representation of the Active-Site Architecture of (A) *M. sativa* CHS, (B) *A. arborescens* PCS, (C) *A. arborescens* OKS, (D) PCS M207G Mutant, and (E) PCS F80A/Y82A/M207G Mutant

The “horizontally restricting” G256L substitution controls the starter substrate selectivity, while the “downward expanding” T197G substitution open a gate to a newly found buried pocket. Residue 338 located next to the catalytic Cys164 at the “ceiling” of the cavity guides the course of polyketide chain elongation (numbering in *M. sativa* CHS). F80 and Y82 form the bottom face of the buried pocket.

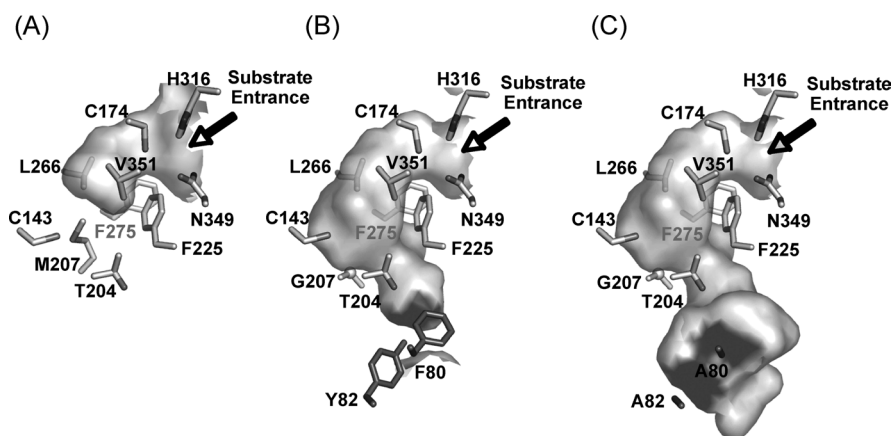


Fig. 9. Comparison of the Active-Site Cavities of (A) Wild-Type PCS (PDB Code 2D3M), (B) PCS M207G Mutant (PDB Code 2D52), and (C) PCS F80A/Y82A/M207G Mutant (Homology Model)

The total cavity volumes are calculated to be 247, 649, and 1031 Å³, respectively.

lining the active-site cavity are perfectly conserved in the mutant, and that the active site of the mutant contains additional novel buried pockets that extend into the traditional active-site cavity (Fig. 9B).⁴⁸ Thus the bulky Met207 blocks the entrance of the pockets in the wild-type PCS, while the large-to-small M207G substitution opens a gate to the buried pockets, thereby expanding the putative polyketide chain elongation tunnel. As we have anticipated, the single-amino acid substitution dramatically increases the volume of the active-site cavity; the total cavity volume of the M207G mutant is 649 Å³, which is 2.6-fold larger than that of the wild-type PCS (247 Å³), and almost as large as that of *M. sativa* CHS (754 Å³). The active-site cavity of the point mutant is now large enough to perform the iterative condensations of eight molecules of malonyl-CoA and to accommodate the octaketide products. These observations clearly support our proposal that the octaketide-producing activity of PCS M207G mutant is totally dependent upon the presence of the additional buried pockets and that the growing linear polyketide intermediates extend into these newly found pockets behind the active site of the enzyme.

Residue 338 (numbering in *M. sativa* CHS) located next to catalytic Cys164 at the “ceiling” of the active-site cavity is also important for the polyketide formation reactions (Fig. 8).^{32,50} Recently, structural analyses of *Pinus sylvestris* STS have led to the proposal that the so-called aldol-switch hy-

drogen bond network involving Ser338-H₂O-Thr132-Glu192 (numbering in *M. sativa* CHS) plays a critical role in the determination of product specificity.¹⁸ Thus, Noel and Schröder proposed that electronic effects, rather than steric factors, balance the competing cyclization specificities in CHS (Claisen type) and STS (aldol type) from a common tetraketide intermediate.¹⁸ Interestingly, however, the conserved Ser338 of CHS is uniquely substituted with hydrophobic Val351 in both PCS and OKS, and such a hydrogen bond network is not observed in the crystal structures. We propose that the hydrophobic Val351 in PCS and OKS provides steric guidance so that the linear polyketide intermediate extends into the newly found downward expanding pocket, thereby leading to the formation of the pentaketide and the octaketide products, respectively. To our surprise, it has recently been demonstrated that the S338V point mutation of *Scuterallia baicalensis* CHS produced a trace amount of the octaketides SEK4/SEK4b in addition to the predominant product TAL.⁵⁰ Moreover, the octaketide-forming activity was dramatically increased in an OKS-like triple mutant (T197G/G256L/S338V) of *S. baicalensis* CHS. More intriguingly, close examination of the published crystal structure of *M. sativa* CHS⁴ revealed the presence of the additional buried pocket that extends into the “floor” of the traditional CHS active site. It is remarkable that CHS, the ubiquitous plant type III PKS, can be easily engineered to produce

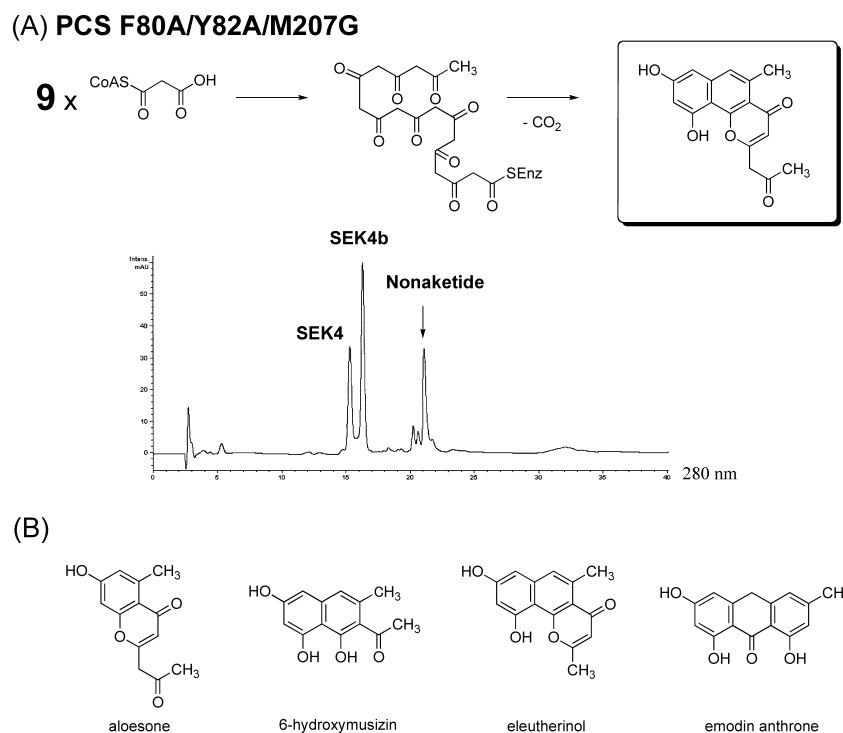


Fig. 10. (A) Enzyme Reaction and HPLC Elution Profile of *A. arborescens* PCS F80A/Y82A/M207G Mutant and (B) Structures of Closely Related Aromatic Polyketides

the octaketides SEK4/SEK4b by such a simple steric modulation of the active-site cavity.

Finally, the conserved G256 of CHS (numbering in *M. sativa* CHS) located at the so-called coumaroyl binding pocket⁴⁾ is uniquely replaced with Leu266 in both *A. arborescens* PCS and OKS, just as in the case of *G. hybrida* 2PS.^{37,38)} This substitution causes the loss of the CHS's coumaroyl-binding pocket from the active-site of PCS and OKS. This “horizontally restricting” bulky G256L substitution (numbering in *M. sativa* CHS) is thus thought to contribute to a steric constriction of the coumaroyl binding pocket, controlling the starter substrate selectivity. As a result, both PCS and OKS no longer accept the *p*-coumaroyl-CoA as a starter substrate to produce chalcone but instead efficiently accept the smaller malonyl-CoA starter to initiate the iterative condensation reactions (Fig. 8).

6. Structure-Based Engineering

As described above, the pentaketide-producing *A. arborescens* PCS was functionally transformed into an octaketide-forming enzyme by the simple steric modulation of the chemically inert single residue 207 lining the active-site cavity. To engineer the PCS enzyme reaction further, we expanded the polyketide elongation tunnel of the M207G mutant by simultaneously substituting two aromatic residues, Phe80 and Tyr82, located at the bottom of the newly found buried pocket, with small Ala (Fig. 8E).⁵¹⁾ A homology model on the basis of the crystal structure of the PCS M207G mutant predicted that the total cavity volume of the F80A/Y82A/M207G triple mutant (1031 Å³) is 4-fold larger than that of the wild-type PCS (247 Å³) (Fig. 9C).

As we had expected, the PCS triple mutant afforded an unnatural novel nonaketide naphthopyrone (0.2% yield, 10-

fold less efficient than that of the pentaketide formation by the wild-type enzyme) in addition to octaketides SEK4/SEK4b (Fig. 10).⁵¹⁾ Interestingly, the structure of the angular nonaketide naphthopyrone showed close similarity to those of heptaketides aloesone and 6-hydroxymusizin from *R. palmatum*,⁵²⁾ and an octaketide eleutherinol isolated from another medicinal plant *Eleutherine bulbosa* (Iridaceae),⁵³⁾ which suggested that these aromatic polyketides are also produced by closely related type III PKS superfamily enzymes (Fig. 10B). On the other hand, it should be noted that the structure of the newly generated angular naphthopyrone is apparently different from that of the pentaketide chromon, the normal product of PCS.

Remarkably, the PCS F80A/Y82A/M207G mutant not only catalyzed the iterative condensation of nine molecules of malonyl-CoA but also altered the mechanism of the cyclization to produce the angular naphthopyrone with a fused tricyclic ring system. Most of the reactions were, however, terminated at the octaketide stage to afford SEK4/SEK4b as major products. Further optimization of the active-site architecture would lead to improvement of the yield of the unnatural novel product. On the other hand, despite the structural similarity to eleutherinol, formation of the “octaketide” naphthopyrone was not detected with either the M207G point mutant or the triple mutant, suggesting that the naphthalene ring-forming activity was only achieved with the F80A/Y82A/M207G triple mutation.

The proposed mechanism of the formation of the nonaketide naphthopyrone involves a sequential C–C bond formation by intramolecular aldol-type condensations (Fig. 11A).⁵¹⁾ It is likely that the enzyme catalyzes the first aromatic ring formation reaction from a linear nonaketide intermediate. After the C–S thioester bond cleavage from the cat-

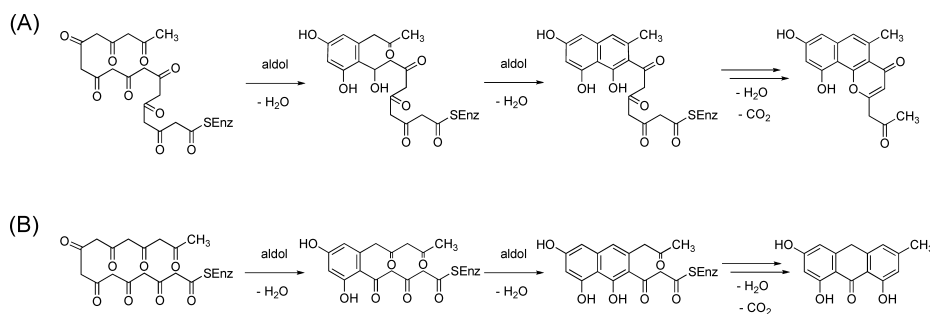


Fig. 11. Proposed Mechanism of the Formation of (A) the Naphthopyrone and (B) Emodin Anthrone from Linear Polyketide Intermediates

alytic Cys174, the partially cyclized aromatic intermediates would then be released from the active site and undergo subsequent spontaneous cyclizations, thereby producing the fused tricyclic ring system. Interestingly, Harris and coworkers previously reported chemical syntheses of polycyclic polyketides; β -polyketones having the two terminal carbonyl groups protected as ketals are efficiently and directly cyclized into aromatic polyketides including 6-hydroxymusizin and eleutherinol.^{54,55} Finally, the formation of the nonaketide naphthopyrone by the *A. arborescens* PCS mutant again strongly suggests the involvement of the CHS superfamily type III PKSs in the biosynthesis of anthrones and anthraquinones in the aloe plant (Fig. 11B).⁵¹

7. Conclusions and Future Directions

A. arborescens PCS and OKS are novel plant-specific type III PKSs that produce pentaketide 5,7-dihydroxy-2-methylchromone and octaketides SEK4/SEK4b, respectively. In the two enzymes, the conserved CHS active-site residues are uniquely substituted with T197M/G256L/S338V in PCS and T197G/G256L/S338V in OKS (numbering in *M. sativa* CHS), thereby controlling the substrate and product specificities of the enzymes. Site-directed mutagenesis and X-ray crystallographic studies clearly demonstrated that the chemically inert single residue 197 determines the polyketide chain length and the product specificity. It is remarkable that the functional diversity of the type III PKSs evolved from the simple steric modulation of the active-site architecture. These findings revolutionized our concept of the catalytic potential of the structurally simple type III PKSs and suggested their involvement in the biosynthesis of structurally diverse plant polyketides such as anthrones and anthraquinones. Further analyses of the catalytic potential and plasticity of the functionally divergent CHS superfamily type III PKSs promise to reveal intimate structural details of the enzyme-catalyzed processes. There are still many fundamental questions on enzyme mechanisms remaining to be elucidated.

On the basis of the crystal structures of both wild-type and M207G mutant PCS, a triple mutant PCS F80A/Y82A/M207G was constructed and shown to catalyze iterative condensations of nine molecules of malonyl-CoA to produce a novel nonaketide naphthopyrone. Structure-based engineering of the type III PKS superfamily enzymes would thus lead to further production of chemically and structurally divergent novel polyketides. Since we can now manage to control the starter substrate specificity and the number of the malonyl-CoA condensations, the next goal is how to regulate the mechanism of the cyclization reactions to generate polyke-

tides with the desired ring systems.

On the other hand, the β -polyketo intermediates are known to be highly reactive and readily react with amines to form Schiff bases, which make it possible to induce more complex chemical reactions such as Mannich-type cyclization. Therefore a combination of i) a protein engineering approach by manually arranging basic residues at the active-site center of the enzyme, and ii) precursor-directed biosynthetic methodology utilizing rationally designed nitrogen-containing synthetic substrate analogues is expected to generate unnatural novel polyketide-alkaloid scaffolds with promising biological activities, which is now in progress in our laboratories.

Acknowledgments I would like to express sincere appreciation to an excellent group of coworkers whose contributions are cited in the text, in particular to Dr. Hiroyuki Morita (University of Shizuoka), Professor Hiroshi Noguchi (University of Shizuoka), and Dr. Toshiyuki Kohno (Mitsubishi Kagaku Institute of Life Sciences). Financial support at the University of Shizuoka has been provided by the PRESTO program of the Japan Science and Technology Agency, and a Grant-in-Aid for Scientific Research from the Ministry of Education, Culture, Sports, Science and Technology, Japan.

References

- Schröder J., "Comprehensive Natural Products Chemistry," Vol. 2, Elsevier, Oxford, 1999, pp. 749–771.
- Austin M. B., Noel J. P., *Nat. Prod. Rep.*, **20**, 79–110 (2003).
- Staunton J., Weissman K. J., *Nat. Prod. Rep.*, **18**, 380–416 (2001).
- Ferrer J. L., Jez J. M., Bowman M. E., Dixon R. A., Noel J. P., *Nat. Struct. Biol.*, **6**, 775–784 (1999).
- Jez J. M., Ferrer J. L., Bowman M. E., Dixon R. A., Noel J. P., *Biochemistry*, **39**, 890–902 (2000).
- Jez J. M., Noel J. P., *J. Biol. Chem.*, **275**, 39640–39646 (2000).
- Jez J. M., Bowman M. E., Noel J. P., *Biochemistry*, **40**, 14829–14838 (2001).
- Jez J. M., Bowman M. E., Noel J. P., *Proc. Natl. Acad. Sci. U.S.A.*, **99**, 5319–5324 (2002).
- Tropf S., Kärcher B., Schröder G., Schröder J., *J. Biol. Chem.*, **270**, 7922–7928 (1995).
- Suh D. Y., Fukuma K., Kagami J., Yamazaki Y., Shibuya M., Ebizuka Y., Sankawa U., *Biochem. J.*, **350**, 229–235 (2000).
- Suh D. Y., Kagami J., Fukuma K., Sankawa U., *Biochem. Biophys. Res. Commun.*, **275**, 725–730 (2000).
- Abe I., Morita H., Nomura A., Noguchi H., *J. Am. Chem. Soc.*, **122**, 11242–11243 (2000).
- Morita H., Takahashi Y., Noguchi H., Abe I., *Biochem. Biophys. Res. Commun.*, **279**, 190–195 (2000).
- Abe I., Takahashi Y., Noguchi H., *Org. Lett.*, **4**, 3623–3626 (2002).
- Abe I., Takahashi Y., Lou W., Noguchi H., *Org. Lett.*, **5**, 1277–1280 (2003).
- Abe I., Watanabe T., Noguchi H., *Phytochemistry*, **65**, 2447–2453 (2004).
- Oguro S., Akashi T., Ayabe S., Noguchi H., Abe I., *Biochem. Biophys. Res. Commun.*, **325**, 561–567 (2004).
- Austin M. B., Bowman M. E., Ferrer J.-L., Schröder J., Noel J. P.,

- Chem. Biol.*, **11**, 1179—1194 (2004).
- 19) Morita H., Noguchi H., Schröder J., Abe I., *Eur. J. Biochem.*, **268**, 3759—3766 (2001).
- 20) Lukacin R., Springob K., Urbanke C., Ernwein C., Schröder G., Schröder J., Matern U., *FEBS Lett.*, **448**, 135—140 (1999).
- 21) Lukacin R., Schreiner S., Matern U., *FEBS Lett.*, **508**, 413—417 (2001).
- 22) Wanibuchi K., Zhang P., Abe T., Morita H., Kohno T., Chen G., Noguchi H., *FEBS J.*, **274**, 1073—1082 (2007).
- 23) Morita H., Kondo S., Kato R., Wanibuchi K., Noguchi H., Sugio S., Abe I., Kohno T., *Acta Crystallogr.*, **F63**, 576—587 (2007).
- 24) Abe I., Takahashi Y., Morita H., Noguchi H., *Eur. J. Biochem.*, **268**, 3354—3359 (2001).
- 25) Abe I., Sano Y., Takahashi Y., Noguchi H., *J. Biol. Chem.*, **278**, 25218—25226 (2003).
- 26) Abe I., Abe T., Wanibuchi K., Noguchi H., *Org. Lett.*, **8**, 6063—6065 (2006).
- 27) Abe T., Morita H., Noma H., Kohno T., Noguchi H., Abe I., *Bioorg. Med. Chem. Lett.*, **17**, 3161—3166 (2007).
- 28) Morita H., Tanio M., Kondo S., Kato R., Wanibuchi K., Noguchi H., Sugio S., Abe I., Kohno T., *Acta Crystallogr.*, **F64**, 304—306 (2008).
- 29) Eckermann S., Schröder G., Schmidt J., Strack D., Edrada R. A., Helariutta Y., Elomaa P., Kotilainen M., Kilpeläinen I., Proksch P., Teeri T. H., Schröder J., *Nature (London)*, **396**, 387—390 (1998).
- 30) Jez J. M., Austin M. B., Ferrer J., Bowman M. E., Schröder J., Noel J. P., *Chem. Biol.*, **7**, 919—930 (2000).
- 31) Abe I., Utsumi Y., Oguro S., Noguchi H., *FEBS Lett.*, **562**, 171—176 (2004).
- 32) Abe I., Watanabe T., Lou W., Noguchi H., *FEBS J.*, **273**, 208—218 (2006).
- 33) Funa N., Ohnishi Y., Fujii I., Shibuya M., Ebizuka Y., Horinouchi S., *Nature (London)*, **400**, 897—899 (1999).
- 34) Funa N., Ohnishi Y., Ebizuka Y., Horinouchi S., *J. Biol. Chem.*, **277**, 4628—4635 (2002).
- 35) Funa N., Ohnishi Y., Ebizuka Y., Horinouchi S., *Biochem. J.*, **367**, 781—789 (2002).
- 36) Austin M. B., Izumikawa M., Bowman M. E., Udway D. W., Ferrer J.-L., Moore B. S., Noel J. P., *J. Biol. Chem.*, **279**, 45162—45174 (2004).
- 37) Abe I., Utsumi Y., Oguro S., Morita H., Sano Y., Noguchi H., *J. Am. Chem. Soc.*, **127**, 1362—1363 (2005).
- 38) Abe I., Oguro S., Utsumi Y., Sano Y., Noguchi H., *J. Am. Chem. Soc.*, **127**, 12709—12716 (2005).
- 39) Fu H., Ebert-Khosla S., Hopwood D. A., Khosla C., *J. Am. Chem. Soc.*, **116**, 4166—4170 (1994).
- 40) Fu H., Hopwood D. A., Khosla C., *Chem. Biol.*, **1**, 205—210 (1994).
- 41) Abe T., Noma H., Noguchi H., Abe I., *Tetrahedron Lett.*, **47**, 8727—8730 (2006).
- 42) Preisig-Muller R., Gnau P., Kindl H., *Arch. Biochem. Biophys.*, **317**, 201—207 (1995).
- 43) Durbin M. L., Learn G. H. J., Huttley G. A., Clegg M. T., *Proc. Natl. Acad. Sci. U.S.A.*, **92**, 3338—3342 (1995).
- 44) Tropf S., Lanz T., Rensing S. A., Schröder J., Schröder G., *J. Mol. Evol.*, **38**, 610—618 (1994).
- 45) Akiyama T., Shibuya M., Liu H.-M., Ebizuka Y., *Eur. J. Biochem.*, **263**, 834—839 (1999).
- 46) Eckermann C., Schröder G., Eckermann S., Strack D., Schmidt J., Schneider B., Schröder J., *Phytochemistry*, **62**, 271—286 (2003).
- 47) Morita H., Kondo S., Abe T., Noguchi H., Sugio S., Abe I., Kohno T., *Acta Crystallogr.*, **F62**, 899—901 (2006).
- 48) Morita H., Kondo S., Oguro S., Noguchi H., Sugio S., Abe I., Kohno T., *Chem. Biol.*, **14**, 359—369 (2007).
- 49) Morita H., Kondo S., Kato R., Wanibuchi K., Noguchi H., Sugio S., Abe I., Kohno T., *Acta Crystallogr.*, **F63**, 947—949 (2007).
- 50) Abe I., Watanabe T., Morita H., Kohno T., Noguchi H., *Org. Lett.*, **8**, 499—502 (2006).
- 51) Abe I., Morita H., Oguro S., Noma H., Wanibuchi K., Kawahara N., Goda Y., Noguchi H., Kohno T., *J. Am. Chem. Soc.*, **129**, 5976—5980 (2007).
- 52) Tsuboi M., Minami M., Nonaka G., Nishioka I., *Chem. Pharm. Bull.*, **25**, 2708—2712 (1977).
- 53) Birch A. J., Donovan F. W., *Aust. J. Chem.*, **6**, 373—378 (1953).
- 54) Harris T. M., Wittek P. J., *J. Am. Chem. Soc.*, **97**, 3270—3271 (1975).
- 55) Harris T. M., Harris C. M., *Pure Appl. Chem.*, **58**, 283—294 (1986).